British Journal of Pharmacology (2008) 155, 957–966

0007–1188/08 $32.00
www.brjpharmacol.org

RESEARCH PAPER

Pharmacology of the short QT syndrome N588K-hERG K^+ channel mutation: differential impact on selected class I and class III antiarrhythmic drugs

MJ McPate, RS Duncan, JC Hancox and HJ Witchel[1]

Cardiovascular Research Laboratories, Department of Physiology and Pharmacology, School of Medical Sciences, University of Bristol, Bristol, UK

Background and purpose: The short QT syndrome (SQTS) is associated with cardiac arrhythmias and sudden death. The SQT1 form of SQTS results from an inactivation-attenuated, gain-of-function mutation (N588K) to the *human ether-à-go-go-related gene* (hERG) potassium channel. Pharmacological blockade of this mutated hERG channel may have therapeutic value. However, hERG-blocking potencies of canonical inhibitors such as E-4031 and D-sotalol are significantly reduced for N588K-hERG. Here, five hERG-blocking drugs were compared to determine their relative potencies for inhibiting N588K channels, and two other inactivation-attenuated mutant channels were tested to investigate the association between impaired inactivation and altered drug potency.
Experimental approach: Whole-cell patch clamp measurements of hERG current (I_{hERG}) mediated by wild-type and mutant (N588K, S631A and N588K/S631A) channels were made at 37 °C CHO cells.
Key results: The N588K mutation attenuated I_{hERG} inhibition in the following order: E-4031 > amiodarone > quinidine > propafenone > disopyramide. Comparing the three inactivation mutants, the two single mutations, although occurring in different modules of the channel, attenuated inactivation to a nearly identical degree, whereas the double mutant caused considerably greater attenuation, permitting the titration of inactivation. Attenuation of channel inhibition was similar between the single mutants for each drug, and was significantly greater with the double mutant.
Conclusions and implications: The degree of drug inhibition of hERG channels may vary based on the level of channel inactivation. Drugs previously identified as useful for treating SQT1 have the least dependence on hERG inactivation. In addition, our findings indicate that amiodarone may warrant further investigation as a potential treatment for SQT1.
British Journal of Pharmacology (2008) **155,** 957–966; doi:10.1038/bjp.2008.325; published online 25 August 2008

Keywords: hERG; *human ether-à-go-go*-related gene; I_{Kr}; inactivation; *KCNH2*; $K_V11.1$; N588K; QT interval; rapid delayed rectifier potassium current; short QT syndrome; SQTS

Abbreviations: I_{Kr}, the 'rapid' delayed rectifier potassium current; SQT1, the form of short QT syndrome associated with the N588K mutation of hERG; SQTS, short QT syndrome; WT, wild type

Introduction

The short QT syndrome (SQTS) is a recently identified condition associated with shorter QT intervals on the ECG and with an increased incidence of cardiac arrhythmias and of sudden death (Gussak *et al.*, 2000, 2002; Gaita *et al.*, 2003; Schimpf *et al.*, 2005). The SQTS is genetically heterogeneous: since 2004, several gain-of-function mutations have been reported in the *KCNH2*, *KCNQ1* and *KCNJ2* K^+ channel genes (Bellocq *et al.*, 2004; Brugada *et al.*, 2004; Hong *et al.*, 2005a, b; Priori *et al.*, 2005). The SQT1 variant is caused by a single amino-acid residue substitution (asparagine-to-lysine; N588K) in the turret (also called the S5-pore linker) region of *KCNH2*-encoded hERG potassium channels (Brugada *et al.*, 2004; Hong *et al.*, 2005a). The *human ether-à-go-go-related gene* (*hERG*) encodes the pore-forming α-subunit of the channel that mediates the rapid delayed rectifier potassium current (I_{Kr}), which is important for action potential repolarization in cardiomyocytes.

The SQT1 hERG mutation leads to impaired I_{Kr} inactivation over the physiological range of membrane potentials, resulting in increased I_{Kr}, and thus accelerated ventricular repolarization (Brugada *et al.*, 2004; Cordeiro *et al.*, 2005; McPate *et al.*, 2005). Currently in SQTS patients, the use of implantable cardioverter defibrillators can help prevent episodes of ventricular fibrillation, but the use of implantable cardioverter defibrillators carries an increased risk of

Correspondence: Professor JC Hancox or Dr HJ Witchel, Cardiovascular Research Laboratories, Department of Physiology, School of Medical Sciences, University of Bristol, Bristol BS8 1TD, UK.
E-mails: jules.hancox@bristol.ac.uk or h.witchel@bsms.ac.uk
[1]Current address: Brighton and Sussex Medical School, University of Sussex, Falmer BN1 9PX, UK.
Received 25 February 2008; revised 9 June 2008; accepted 17 July 2008; published online 25 August 2008

inappropriate shocks due to T-wave oversensing in some patients (Schimpf *et al.*, 2003). Therefore, decreasing the I_{Kr} current in SQT1 patients by using drugs that either block N588K-hERG or restore its inactivation could offer an attractive adjunct to the use of implantable cardioverter defibrillators.

The wild-type (WT) hERG channel is blocked by a wide range of structurally and pharmacologically diverse agents (Redfern *et al.*, 2003; Witchel, 2007). The majority of such agents prolong the QT interval in animals and normal volunteers when used at high concentrations. For most of these agents, these are off-target effects, and hERG's lack of specificity has led to the channel's drug interactions being described as 'promiscuous' (for a review see Witchel, 2007). The search for drugs to correct SQT1 began inauspiciously when some highly specific hERG blockers in the methanesulphonanilide class were found to be relatively ineffective at correcting the QT interval, including the class III antiarrhythmic drugs sotalol (Brugada *et al.*, 2004) and ibutilide (Gaita *et al.*, 2004). In addition, the methanesulphonanilide D–sotalol (Brugada *et al.*, 2004) and the high-affinity hERG blocker E-4031 (McPate *et al.*, 2006) were attenuated in their ability to inhibit the cellular currents mediated by the SQT1 mutant of hERG (N588K). Thus, the SQT1 variant of hERG not only causes an increase in whole-cell current mediated by the channel but also seems to interfere with the ability of some drugs to block the channel and thus correct the QT interval in affected individuals (Brugada *et al.*, 2004; Wolpert *et al.*, 2005).

By contrast, the class Ia antiarrhythmic quinidine can be used to treat SQT1, and quinidine corrects the QT interval (a marker of risk) as well as blocking N588K with only fivefold attenuated potency compared with its inhibition of WT hERG (Wolpert *et al.*, 2005). Propafenone has also been shown to reduce the risk of SQT1-associated atrial fibrillation (Hong *et al.*, 2005a), although it does not correct the QT interval, either because propafenone is ineffective against N588K-hERG or possibly due to the known calcium channel-blocking activity of propafenone (Delgado *et al.*, 1993; Hancox and Mitcheson, 1997) offsetting propafenone's hERG-blocking properties, thereby preventing prolongation of the action potential and QT interval duration.

Our recent research suggested that the low-affinity hERG blocker disopyramide, which blocks N588K I_{hERG} with little alteration to its potency, would be an attractive agent to investigate further for use with SQT1 (McPate *et al.*, 2006), and a subsequent pilot study testing this hypothesis on patients suggests that this strategy may have some clinical merit (Schimpf *et al.*, 2007). In this study, we demonstrate—using a range of drugs—that SQT1 may be more responsive at therapeutic concentrations to those hERG blockers that do not depend strongly on inactivation for their potency.

Methods

Maintenance of cells expressing WT and mutant hERG channels
Whole-cell patch clamp recordings were made from Chinese hamster ovary cells expressing hERG (McPate *et al.*, 2005). Briefly, wild-type hERG (alternative nomenclature $K_V11.1$; Alexander *et al.*, 2008) was stably transfected into Chinese hamster ovary cells. The N588K-hERG mutation was generated using a Quikchange II XL site-directed mutagenesis kit (Stratagene, La Jolla, CA, USA) (McPate *et al.*, 2005). The S631A mutation was generated as previously described (Hancox *et al.*, 1998). The double mutant was made using a two primer strategy incorporating the S631A mutation in the antisense primer (beginning at the fortuitous unique *Bgl*II restriction site) while using the N588K plasmid as the template. The media used, transfections and the creation of stable cell lines have been described previously (Milnes *et al.*, 2003; McPate *et al.*, 2005).

Electrophysiological recordings
Glass coverslips containing cells were placed in a bath mounted on an inverted microscope and continuously superfused (at 37 °C) with Tyrode's solution containing (in mM): 140 NaCl, 4 KCl, 2.5 $CaCl_2$, 1 $MgCl_2$, 10 glucose and 5 HEPES (titrated to pH 7.45 with NaOH). Patch pipettes (Corning 7052 glass; AM Systems, Carlsborg, WA, USA) pulled and heat polished (Narishige MF83) to 2.2–4.8 MΩ were filled with a solution containing (in mM): 130 KCl, 1 $MgCl_2$, 5 EGTA, 5 MgATP and 10 HEPES (titrated to pH 7.2 using KOH). Equipment, data digitization and recording were as described previously (McPate *et al.*, 2005).

Data analysis
Data were analysed using Clampex 8.2 (Axon Instruments now trading as Molecular Devices, Wokingham, Berkshire, UK), Excel 2003, Instat (GraphPad Inc., La Jolla, CA, USA) and Prism v3.02 (GraphPad Inc.) software. Data are presented as mean ± s.e.mean, or as mean and 95% confidence interval. Statistical analysis was performed using a one-way ANOVA (Prism v3). *P*-values of less than 0.05 were taken as statistically significant.

Fractional block of I_{hERG} was calculated using the following equation:

$$\text{Fractional block} = 1 - \left(\frac{I_{\text{hERG-drug}}}{I_{\text{hERG-control}}}\right) \quad (1)$$

where $I_{\text{hERG-control}}$ is the whole-cell peak tail current of hERG under the conditions listed, and $I_{\text{hERG-drug}}$ is the peak tail current of that cell under the same conditions after superfusion of drug; tail current is used to quantify the current mediated by the mutant channels as well as WT. The relationship between drug concentration and current block by each drug was determined by fitting data with the Hill equation of the form:

$$\text{Fractional block} = \frac{1}{\left(1 + \left(\frac{IC_{50}}{[\text{drug}]^h}\right)\right)} \quad (2)$$

where IC_{50} is the concentration of drug producing half-maximal inhibition of the I_{hERG} and h is the Hill coefficient for the fit.

The voltage dependence of peak tail currents was fitted to a modified Boltzmann equation of the form:

$$I = \frac{I_{\text{Max}}}{1 + \exp\left(\frac{(V_{0.5} - V_m)}{k}\right)} \quad (3)$$

where I = the normalized I_{hERG} tail peak amplitude upon repolarization following a 2-s depolarizing test potential to

V_m, I_{Max} = the normalized maximal I_{hERG} tail amplitude observed (that is, 1), $V_{0.5}$ = potential at which I_{hERG} tail amplitude was half maximal and k = the slope factor describing I_{hERG} tails. The voltage dependence of availability was determined by fitting the normalized and corrected values of the second depolarization-induced peak currents following depolarization and brief repolarization with a modified Boltzmann of the same form (Equation (3) where I = the corrected I_{hERG} amplitude upon depolarization following a brief repolarizing test potential to V_m, I_{Max} = the maximally available I_{hERG} observed, $V_{0.5}$ = potential at which I_{hERG} was half maximally available and k = the slope factor describing I_{hERG} availability.

Drugs

Disopyramide (Sigma-Aldrich, Gillingham, Dorset, UK), quinidine (Sigma) and E-4031 (generously donated by Eisai, Tokyo, Japan) were dissolved in distilled water to produce required stock solutions. Propafenone (Sigma) was prepared in ethanol at a concentration of 100 mM and serially diluted, ensuring a vehicle concentration of 0.1% at all times. Amiodarone (Sigma) was dissolved in dimethyl sulphoxide at a concentration of 50 mM and then diluted to produce further stock concentrations. Stock solutions were diluted 1:1000 in Tyrode's solution to give final experimental concentrations. Fresh solutions were made on each experimental day.

During recordings, all solutions were applied to the cells under study using a home-built, warmed, multi-barrelled solution application device (Levi *et al*., 1996) capable of changing the bathing solution surrounding a cell in <1 s. Addition of drugs was accompanied by continuous application of a standard hERG voltage command protocol (see Results) with a start-to-start interval of 12 s to allow the channels to achieve an open/inactivated conformation. Amiodarone and E-4031 were slow to reach steady-state block, so concentration–response data were obtained at 10 min, whereas quinidine, disopyramide and propafenone acted more rapidly, enabling concentration–response data to be obtained at 3 min.

Results

Validation and comparison of inactivation of mutant channels

Both of the hERG mutations N588K (Cordeiro *et al*., 2005; McPate *et al*., 2005) and S631A (Hancox *et al*., 1998; Zou *et al*., 1998) are known to attenuate inactivation and thus increase the whole-cell current mediated by the channel at physiological voltages by shifting rightward the voltage dependence of inactivation; however, the degree of inactivation attenuation caused by these two mutations has never been quantified under identical conditions. The novel double mutant N588K/S631A has not been described before. To compare the overall relationship among voltage, activation and inactivation in these four channels, current–voltage relations were elicited by a protocol with an initial 50-ms step from -80 to -40 mV, which then returned to the holding potential at -80 mV for 50 ms (to quantify the instantaneous leak at -40 mV and then restore the channels to a deactivated state). This was followed by a depolarizing step to a range of test potentials between -40 and $+60$ mV for 2 s, which were followed by observation of tails at -40 mV for 4 s (see Figure 1). For a given test potential, attenuated hERG inactivation would be expected to appear as an increase in the ratio of the current during the depolarizing pulse compared with the tail current (where I_{hERG} tail amplitudes were measured as the difference between peak outward tail current and instantaneous current activated by the 50 ms depolarization from -80 to -40 mV), thus effectively eliminating the paradoxical resurgent tail current (Robertson, 2000). As shown in the representative traces, in the WT channel (Figure 1a) for voltages of -20 mV and above, the current at the end of the 2-s depolarizing step is smaller than the peak tail current at -40 mV, whereas in all three of the mutated channels at these voltages, the current during the pulse is large compared with the peak tail current (Figures 1b–d).

The mean current–voltage ($I-V$) relationships for currents normalized to the largest of the elicited currents at the end of the 2-s depolarizing step (Figure 1e) and for currents at the peak of the tail current (Figure 1f) for S631A and for the N588K/S631A double mutant are accompanied by the data gathered under identical conditions (dashed lines without symbols) for WT and N588K (McPate *et al*., 2005). The rectification of the end pulse current (Figure 1e), compared with WT, is shifted rightward for all three mutants, with the N588K/S631A mutant showing no rectification at all at these voltages. Partial rectification of the N588K/S631A end pulse current was observed only during test potentials to $+80$ and $+100$ mV (data not shown). The mean normalized peak tail current amplitudes (Figure 1f) were fitted with a modified Boltzmann equation (Equation (3)). The half-maximal voltages for activation ($V_{0.5}$) for these fits were -20.1 ± 0.8 mV (WT), -22.4 ± 0.6 mV (N588K), -19.1 ± 1.1 mV (S631A) and -24.7 ± 1.0 mV (N588K/S631A). The slope factors (k) for these fits were 7.9 ± 0.7 (WT), 8.1 ± 0.6 (N588K), 8.7 ± 1.0 (S631A) and 9.0 ± 0.9 (N588K/S631A). The $V_{0.5}$ values for individual cells were pooled for each channel type, then they were analysed using a one-way ANOVA followed by a Bonferroni post-test; this revealed that there was no significant difference in activation $V_{0.5}$ values between the different channel types ($P>0.05$).

To quantify the effects on inactivation, and particularly on the voltage dependence of I_{hERG} availability, command protocols were applied to cells expressing the WT channel where the membrane was depolarized to $+40$ mV for 500 ms (which allowed for $>90\%$ inactivation of the channel), and then the membrane potential was repolarized to a range of potentials from -140 to $+40$ mV in the intervals of 10 mV for 10 ms, before stepping back to $+40$ mV. The elicited peak current during the last step to $+40$ mV following each brief repolarizing voltage step was normalized to the largest induced current for that particular cell. To take into account any capacitative transients that may mask the observed current during the third pulse, the peak currents were fitted with a single exponential function and extrapolated back to the beginning of the third pulse as described previously

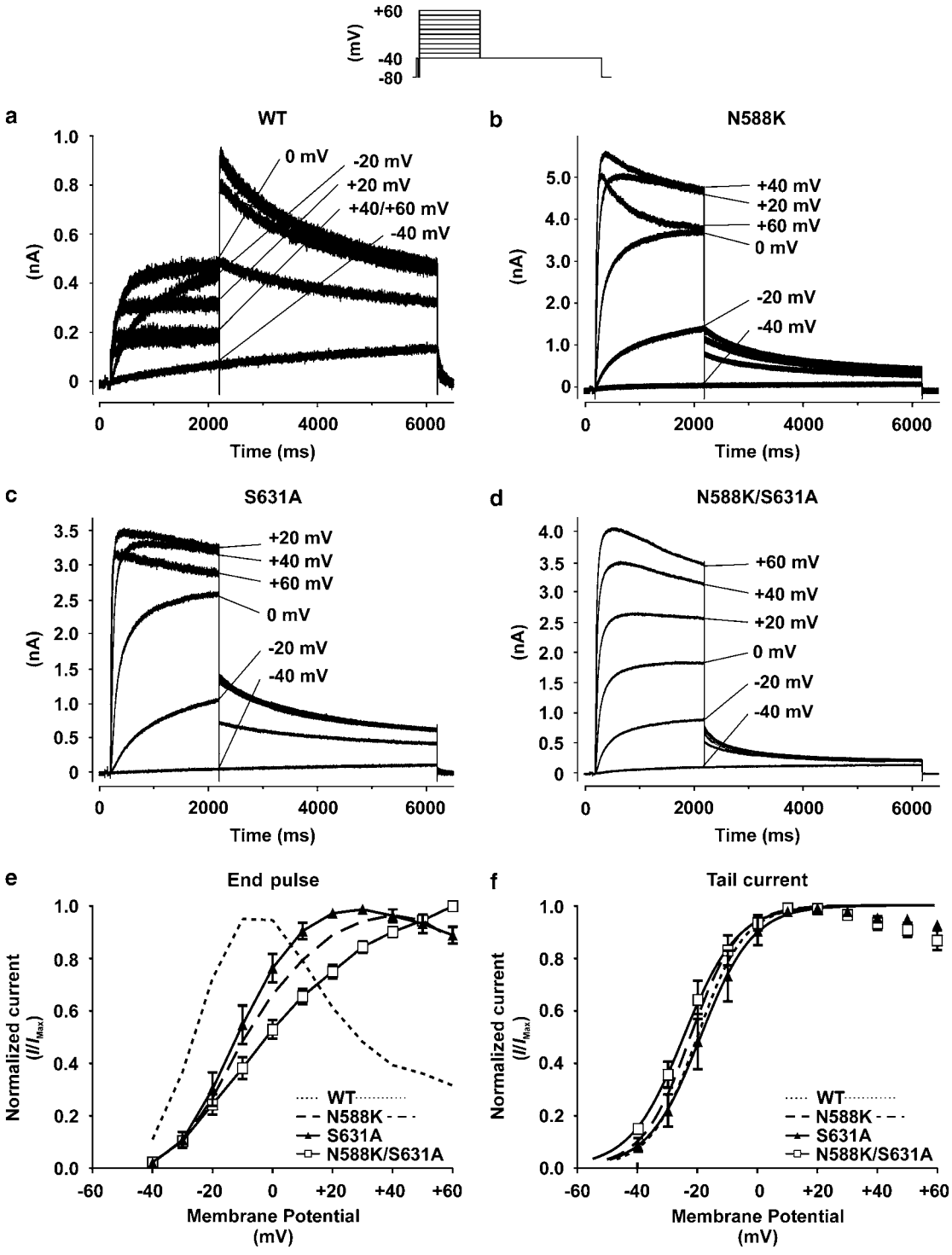

Figure 1 Current–voltage relationships for S631A hERG and for the N588K/S631A hERG double mutant. Representative current traces for wild-type (WT) (**a**), N588K (**b**), S631A (**c**) and the N588K/S631A double mutant (**d**) were elicited by the voltage protocol shown (inset, top); some traces were omitted from the overlaid currents for clarity. For this voltage protocol, the membrane was held at −80 mV, and then a brief 50-ms pulse to −40 mV was applied to allow precise observation of tail current leak (cells with non-zero leak were rejected), the channels were allowed to fully deactivate at −80 mV for 50 ms, and then a depolarizing pulse to a range of potentials between −40 and + 60 mV (in 10-mV increments) for 2 s was applied, followed by the observation of tail currents at −40 mV for 4 s. The start-to-start interval was 12 s. The mean of elicited normalized current (I/I_{max}) at the end of the 2-s depolarizing steps (**e**) and the mean of the normalized peak tail currents (**f**) are shown ($N = 5$ for each); lines representing Boltzmann fits were calculated as per the Methods. Mean data for WT and N588K hERG (McPate *et al.*, 2005) are included for comparison; these plots are represented as dashed lines without symbols.

(Zou *et al*., 1998; Witchel *et al*., 2004; McPate *et al*., 2005). On account of deactivation of channels occurring during the short repolarization steps, the correction method of Smith *et al*. (1996) was also used. The data were fitted to a Boltzmann function (Equation (3)), and from that a $V_{0.5}$ of -58.52 ± 0.77 mV was determined. A similar protocol was used for both N588K and S631A, except that the depolarizing voltage was $+80$ mV and the brief repolarization steps ranged from -100 to $+80$ mV; the increased depolarization was necessary to attain $>90\%$ inactivation. With this protocol, the $V_{0.5}$ values of availability for N588K and S631A-hERG were $+29.96 \pm 0.74$ and $+30.53 \pm 0.73$ mV, respectively ($P>0.05$, one-way ANOVA).

In the process of attempting to measure the availability of the N588K/S631A double mutant, it was noticed that even at $+80$ mV, inactivation was only $27.9 \pm 5.3\%$ ($n=4$), whereas calculating availability is most accurate when starting from a voltage where inactivation is $>90\%$. As these mammalian cells are not readily capable of withstanding lengthy depolarizations to potentials of $+100$ mV or higher, at least under our recording conditions, another methodology was necessary to compare quantitatively the effects of these mutations on inactivation.

Previous studies have measured the inactivation of hERG (as opposed to its recovery from inactivation) by using a brief hyperpolarizing stimulus and assuming that the induced recovery from inactivation is nearly complete, whereas the deactivation during the brief hyperpolarization is negligible in comparison (Smith *et al*., 1996). This approach can be used to quantify directly the degree of hERG inactivation by taking the ratio of the steady-state current at the end of the first depolarization (when both activation and inactivation are at a steady state) to the peak current at the beginning of the second depolarization (when activation is nominally still at steady state from the previous depolarization, whereas inactivation is nominally nil) (Teschemacher *et al*., 1999). Figure 2 compares the inactivation of the four hERG channels at $+20$ mV using a brief hyperpolarization to -100 mV. The data show clearly that there was no significant difference between the attenuation of inactivation in N588K vs S631A-hERG ($P>0.05$; one-way ANOVA followed by Bonferroni post-test), and also that the two mutations together had synergistic effects on hERG inactivation. Note that there are potential limitations to the interpretation of this protocol if the two assumptions above do not hold for the mutant channels. An additional availability protocol showed that for a 2-ms step to -100 mV, inactivation is almost completely relieved for the single mutants; deactivation of N588K at 37 °C has been previously shown to be quite similar to WT (McPate *et al*., 2005). It is also notable that results using this protocol were in good agreement with those using repolarization steps to different voltages (above), supporting similarly altered inactivation for N588K and S631A hERG.

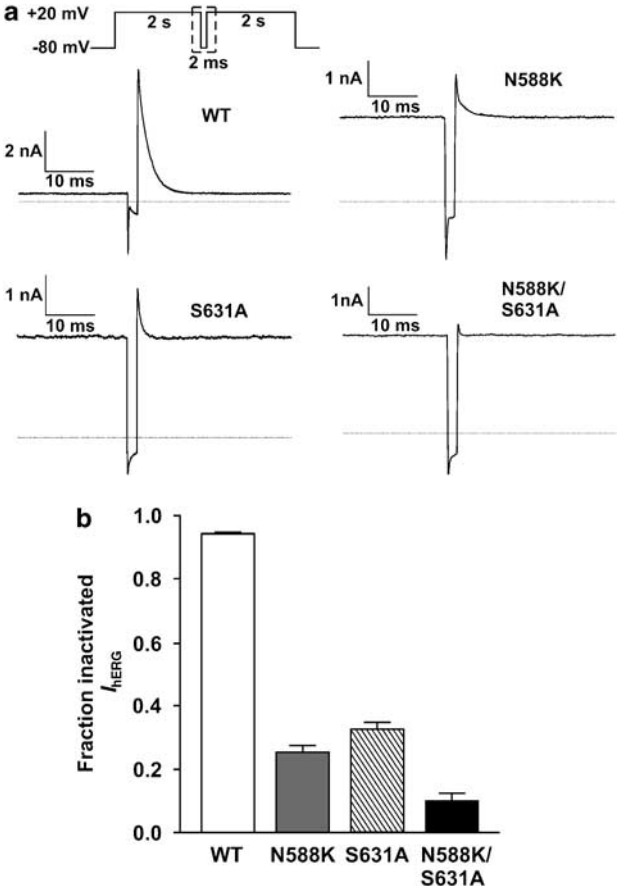

Figure 2 The degree of hERG inactivation for each of the channels at $+20$ mV. To measure the inactivation for the channel, inactivation was isolated from activation by applying a brief (2 ms) hyperpolarizing step to -100 mV (Smith *et al*., 1996). (**a**) Representative traces of the segment of the elicited I_{hERG} from which the fraction of inactivated current for each channel was calculated. The command voltage protocol (inset above) was a step to $+20$ mV for 2 s, inactivation was relieved during a 2 ms hyperpolarization to -100 mV, and then the cells were stepped back to $+20$ mV for 2 s. The cells were held at -80 mV and the start-to-start interval was 12 s. In (**b**) the means of the fraction of steady-state channel current at $+20$ mV that is inactivated was calculated as $1-(I_{inact}/I_{recov})$, where I_{inact} is the current when the channels are at steady-state levels of both activation and inactivation (just before the hyperpolarizing step) and I_{recov} is the peak current just after recovery from inactivation. I_{recov} was estimated by fitting the decaying current elicited just after the beginning of the second step to $+20$ mV with a single exponential fit, and extrapolating the curve to the time point at which the command voltage is stepped from -100 to $+20$ mV; at this point in time, it is estimated that recovery from inactivation is complete and activation is still at steady state for $+20$ mV. $N=5$ cells for each channel. A one-way ANOVA followed by a Bonferroni post-test found that there was a significant difference between the single and double mutants compared with wild-type (WT) hERG ($P<0.001$). There was no significant difference between N588K and S631A-hERG ($P>0.05$), but a significant difference between the single and the double mutants ($P<0.001$).

Drug inhibition of WT hERG and its inactivation mutants

A systematic comparison of the degree of attenuation of blockade by a range of drugs by the two mutants has not been performed previously, nor has there been any previous test for synergistic effects using the double mutant. Figure 3 shows representative current traces elicited by a 'standard' hERG voltage command protocol before and after superfusion of 100 nM E-4031; to perform a standard hERG protocol from a holding potential of -80 mV, after a 50-ms step to -40 mV followed by 50 ms at -80 mV (to quantify

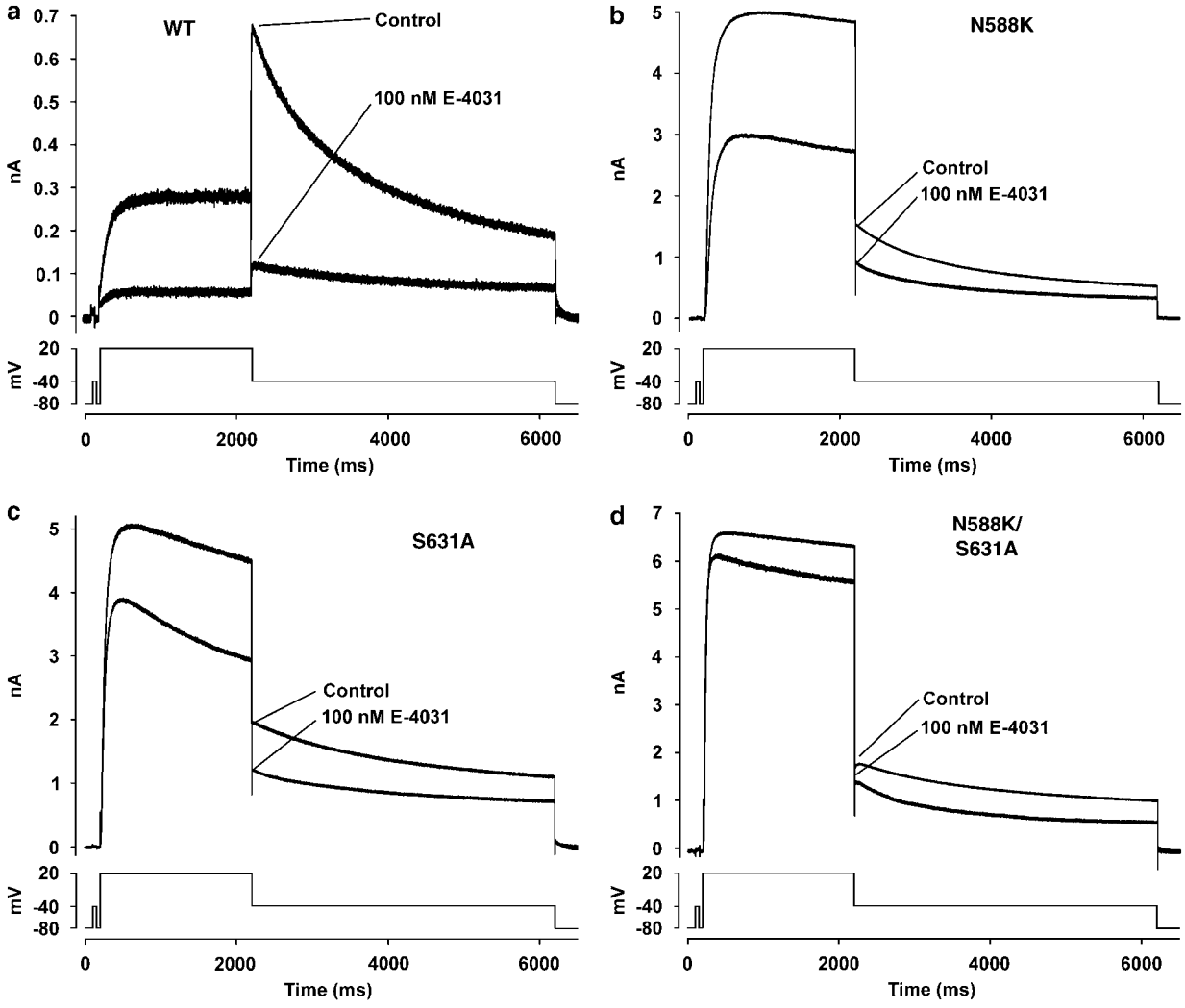

Figure 3 Representative currents of each hERG channel type in the absence and presence of 100 nM E-4031. To compare the effects of the different mutations ((**a**) wild type, (**b**) N588K, (**c**) S631A and (**d**) N588K/631A double mutant) upon high-potency methanesulphonanilide sensitivity, the membranes were subjected to a 'standard' hERG command protocol (see Results) in control solution, and then the cells were superfused with 100 nM E-4031 until the currents reached steady state. The overlaid traces show the elicited I_{hERG} in control superfusate and then at steady state in 100 nM E-4031.

the instantaneous leak at −40 mV and then restore the channels to a deactivated state), the cells were depolarized for 2 s to +20 mV (the voltage for which inactivation had been quantified for the three mutant channels) and then peak tail currents were observed during a 4-s step to −40 mV. Although the inhibition of the peak tail current of WT-hERG under these conditions is >90%, either mutation (N588K or S631A) resulted in reduced inhibition and the double mutant clearly had synergistic effects on reducing the effect of E-4031.

It has been shown previously that the mechanisms by which drugs inhibit the hERG channel have subtle differences; in particular, some hERG blockers can differ in their molecular determinants of blockade from methanesulphonanilides (for example, Milnes *et al*., 2003; Ridley *et al*., 2004). In this study, we have tested a range of drugs: E-4031, which is a high-potency methanesulphonanilide (IC_{50} < 100 nM in mammalian cells at 37 °C (Zhou *et al*., 1998)), propafenone, which has a mid-range potency for hERG (IC_{50} = ~440 nM in mammalian cells (Paul *et al*., 2002)) and a moderate dependence on S631 as a molecular determinant (Witchel *et al*., 2004), quinidine, which has a mid-range potency and little dependence on S631 (Lees-Miller *et al*., 2000; Paul *et al*., 2002), amiodarone, which is unusual in that it has a high potency for hERG inhibition but its blockade is partially resistant to mutations of the canonical molecular determinants of blockade F656 and Y652 (Ridley *et al*., 2004), and disopyramide, which has a low potency for hERG and little sensitivity to mutation of S631 (Paul *et al*., 2001).

Previously, we have shown that the hERG blockade by E-4031 and by disopyramide are differentially affected by the N588K mutation; the mutation increases the IC_{50} for E-4031 by 11.5-fold, but that for disopyramide is increased by only 50% (McPate *et al*., 2006). In Figure 4, we have completed this comparative data set by showing the effects of S631A and the N588K/S631A double mutant in the form of a set of concentration–response curves. For both drugs, the concentration–response curves for N588K and S631A overlie almost precisely and in each case, the double mutant is shown to

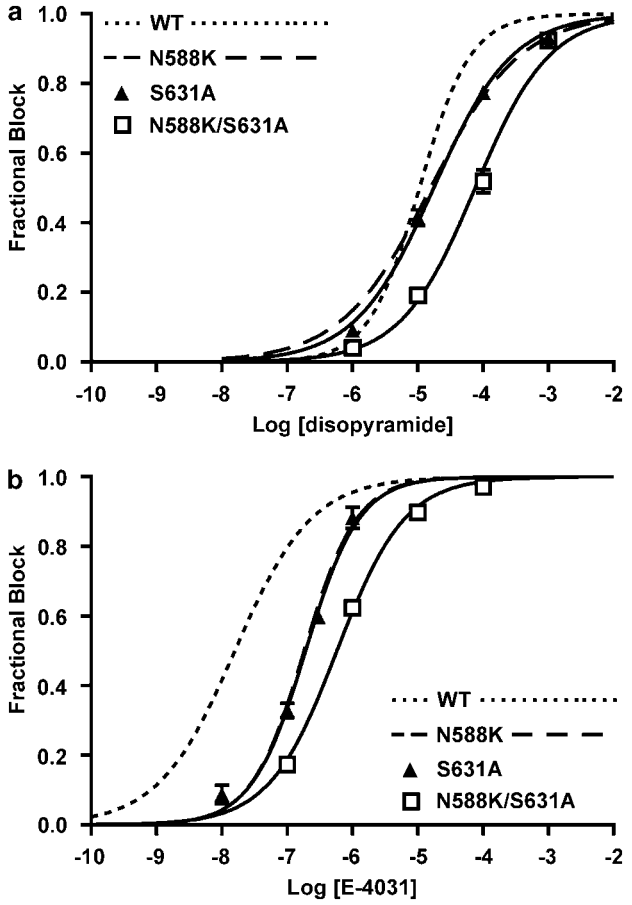

Figure 4 Concentration–response curves for disopyramide and E-4031. The effects of the S631A mutation and the N588K/S631A double mutation on drug sensitivity were compared with previously published data using identical conditions for the wild type (WT) (dotted line plot without symbols) and N588K (dashed line plot without symbols) (McPate *et al*., 2006). Disopyramide (**a**) and E-4031 (**b**) concentration–response curves were obtained using protocols identical to those in Figure 3. Each cell was exposed to only a single drug concentration, and fractional inhibition for that cell was calculated according to Equation (1). Symbols represent the mean fractional inhibition for each drug at each concentration ($N = 5$–10 cells per concentration), and error bars show the s.e.mean. The concentration–response curves were fitted (lines) using Equation (2), which yielded an IC_{50} and Hill coefficient (h) for each drug.

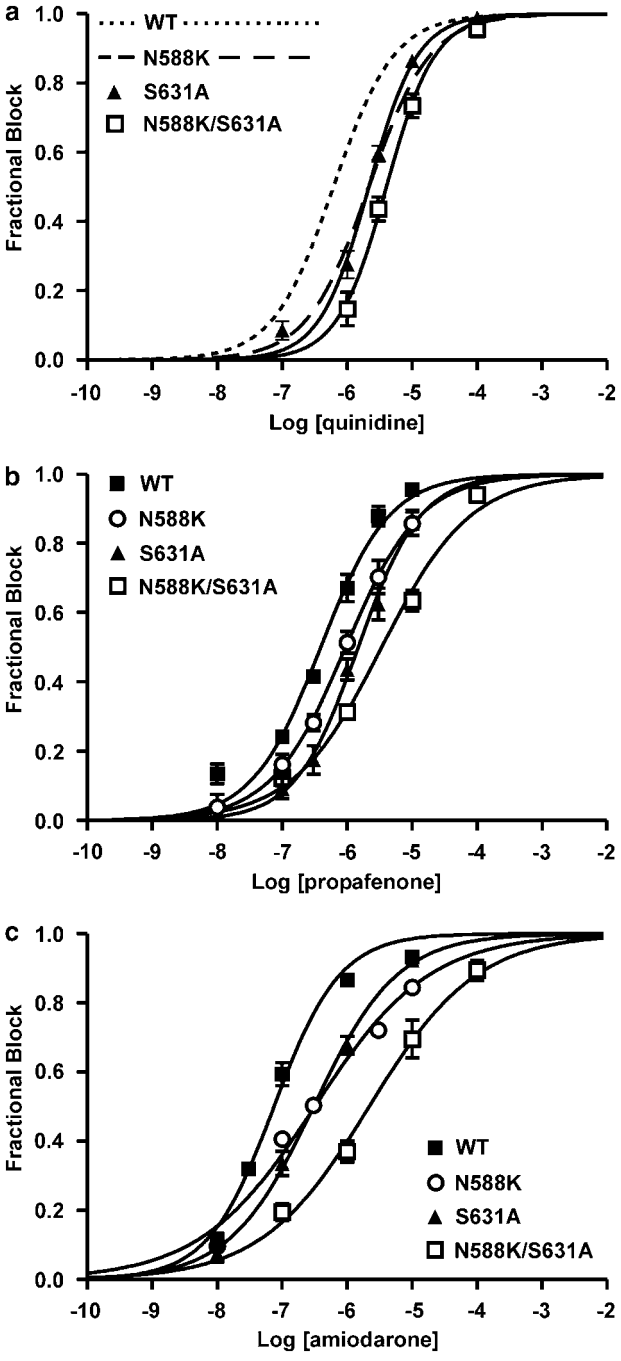

Figure 5 Concentration–response curves for quinidine, propafenone and amiodarone. Concentration–response curves for quinidine (**a**), propafenone (**b**) and amiodarone (**c**) were measured and fitted as in Figure 4. Data for wild-type (WT), N588K, S631A and the N588K/S631A double mutant channels are overlaid. Previous data (McPate *et al*., 2006) for quinidine's effects on the WT (dotted line plot without symbols) and N588K (dashed line plot without symbols) are shown for comparison. $N = 5$ for each drug at each concentration. A one-way ANOVA of the IC_{50} values was performed for each of the drugs. For all three drugs, the IC_{50} values obtained for N588K, S631A and the double mutant were significantly different from WT hERG ($P < 0.001$). There was a slightly significant difference between N588K and S631A for propafenone ($P < 0.05$), but no statistical significance for quinidine and amiodarone ($P > 0.05$). The IC_{50} values for single-mutant channels were significantly different from those for the double mutant, for all three drugs ($P < 0.001$).

have synergistic effects on the concentration–response curves. Concordant with previous observations comparing the effects of these drugs on WT vs N588K, we found E-4031 to be >5-fold more sensitive (as estimated by IC_{50}) to mutations that attenuate inactivation than disopyramide. A one-way ANOVA followed by a Bonferroni post-test was performed on the IC_{50} values for the WT and mutant channels for both E-4031 and disopyramide. For both drugs, the N588K, S631A and N588K/S631A mutations were found to have IC_{50} values that were significantly different when compared with WT hERG ($P < 0.001$), but there was no significant difference between the IC_{50} values for the two single mutants ($P > 0.05$), whereas the double mutant was significantly different from either of the single mutants ($P < 0.001$).

The concentration–response curves of the other three drugs tested were compared in Figure 5. Although the

Table 1 Attenuation of drug inhibition by three inactivation-attenuated mutants compared with wild-type hERG

	IC_{50} in WT-hERG	*Fold decrease in potency relative to WT-hERG (IC_{50} in nM)*		
		S631A	*N588K*	*N588K/S631A*
Disopyramide	10.7 μM (CI: 9.7–11.7)[a]	1.6 (17.58 μM)	1.5 (15.77 μM)[a]	7.1 (75.80 μM)
Quinidine	620 nM (CI: 540–710)[a]	3.5 (2160 nM)	3.5 (2160 nM)[a]	6.5 (4020 nM)
Propafenone	390 nM (CI: 330–380)	3.8 (1490 nM)	2.4 (950 nM)	8.7 (3410 nM)
Amiodarone	75.2 nM (CI: 63.0–89.7)	4.1 (305 nM)	4.2 (318 nM)	29.1 (2190 nM)
E-4031	16.0 nM (CI: 13.3–19.1)[a]	12.0 (192 nM)	11.4 (183 nM)[a]	36.4 (583 nM)

[a]Values obtained previously (McPate *et al*., 2006).
A summary of the concentration–response data in Figures 4 and 5. The IC_{50} values for all five drugs in all four hERG channels were calculated as described and then used in the calculations described below. The IC_{50} values for WT-hERG for all the drugs are shown on the left, and to the right in brackets are the 95% confidence intervals (CIs). To compare the mutations' attenuating effects on inactivation, the decrease in drug potency relative to WT-hERG was calculated for each mutant–drug combination by taking the ratio of the IC_{50} for a particular mutant–drug combination (shown in parentheses) and dividing it by the IC_{50} of the same drug when applied to WT-hERG. The attenuation is expressed as a 'fold decrease in potency', where 1.5 represents a 50% increase in the IC_{50} over WT.

similarity of attenuation of blockade by N588K and S631A is not as striking, for all three drugs, it is clear that both N588K and S631A significantly increased the IC_{50} values ($P<0.001$, when comparing the single mutants against WT hERG for all three drugs; one-way ANOVA followed by Bonferroni post-test). It is also clear that the attenuation of block was similar for the two single mutants, and that the double mutation led to a significant and synergistic effect ($P<0.001$, when comparing the double mutant to each of the single mutants for all three drugs). The effect of the single mutants on the block by propafenone and quinidine (the two mid-range potency blockers) is similar to each other and is greater than the effects of these mutations on disopyramide. There was no significant difference between the two single mutants for amiodarone (a high-potency blocker, $P>0.05$). The single mutations had an increased effect on amiodarone compared with propafenone and quinidine (Table 1), and the double mutant caused a 29-fold decrease in the potency of the block by amiodarone compared with <9-fold for propafenone and quinidine (Table 1). This is concordant with amiodarone's blocking potency being partially resistant to mutations of F656 and Y652 (Ridley *et al*., 2004), and therefore amiodarone's hERG-binding site relating to other conformations inside the pore cavity. A summary of all the drug data concerning blockade of the WT and mutant hERG channels is presented in Table 1, showing the IC_{50} values for the channels for each drug and showing the fraction of blockade that is attenuated for each mutant.

Discussion and conclusions

The main novel conclusions from this study are as follows: (1) The block of hERG by amiodarone is not greatly attenuated by N588K, making it potentially useful for SQT1 treatment; (2) The previously unreported N588K/S631A double mutant results in an expressable channel that has significantly attenuated inactivation compared with either of the N588K or S631A single mutants. (3) In a side-by-side comparison, the N588K and S631A mutations have nearly identical effects in terms of the extent of inactivation attenuation, despite the mutation being in different modules of the channel; (4) For five drugs with unrelated chemical structures, the effects of the three inactivation-attenuating mutations on their hERG inhibition are N588K≅S631A≪N588K/S631A, which is concordant with the order of the mutations' attenuation of hERG inactivation; (5) Drugs can vary to a greater or lesser extent in their overall sensitivities to these three mutations, and the N588K mutation attenuated I_{hERG} inhibition in the following order: E-4031 > amiodarone > quinidine > propafenone > disopyramide.

This study provides the first information regarding the inhibition of the SQT1 mutant channel N588K-hERG by propafenone and amiodarone. Our data indicate that amiodarone, which has been suggested to have value in treating SQTS of unknown phenotype (Lu *et al*., 2006), may be of specific value in SQT1. The evidence for this is that, under identical experimental conditions, the attenuation of amiodarone's potency by the N588K mutation (a 4.2-fold change in IC_{50}) was only slightly less than that for quinidine (3.5-fold), a drug which is known to be effective for SQT1 (Gaita *et al*., 2004; Wolpert *et al*., 2005; Schimpf *et al*., 2007). Presumably, the ability of quinidine (or any other drug) to correct the QT interval and reduce the risk of arrhythmogenesis in SQT1 through a direct effect on hERG depends on its ability to block N588K-hERG at therapeutic concentrations (Brugada *et al*., 2004). Previously, based on single mutation studies, we and others have suggested that quinidine's ability to block N588K-hERG at therapeutic concentrations may derive from its comparative insensitivity to attenuation of hERG inactivation (Brugada *et al*., 2004; Wolpert *et al*., 2005; McPate *et al*., 2006). By making a like-for-like comparison with five drugs and three different mutations, this study strengthens those previous suggestions. The reduced drug potencies found with N588K-hERG are likely to be due to (and certainly correlate with) the inactivation attenuation (whether this be a direct effect on drug binding, or through influencing orientation of binding residues on the S6 helices) rather than to an anomaly in channel structure specifically related to the N588K mutation.

In addition to the present demonstration of this association between drug potency and inactivation with N588K, other investigations of hERG have also posited a similar link (Ficker *et al*., 1998, 2001; Herzberg *et al*., 1998; Yang *et al*., 2004) based on other mutants with attenuated inactivation including G628C/S631C (Mitcheson *et al*., 2000; Numaguchi

et al., 2000; Witchel *et al*., 2004), S631A (Zhang *et al*., 1999; Lees-Miller *et al*., 2000; Witchel *et al*., 2004; Yang *et al*., 2004; Duncan *et al*., 2007) and S620T (Herzberg *et al*., 1998; Ficker *et al*., 2001). These amino-acid residues associated with inactivation are located at three different regions at or near the extracellular face of the channel: the turret, the segment of the outer mouth of the pore that is on the C-terminal side of the pore loop, and within the pore loop. By contrast, to block hERG with high affinity, most such drugs must access the pore cavity from the intracellular side of the channel when the channel is in the activated state, and the canonical high-affinity drug-binding site is strongly associated with two aromatic residues inside the pore cavity in the S6 transmembrane domain: F656 and Y652 (Mitcheson *et al*., 2000). Thus far, there is no accepted general mechanism to explain how inactivation, which depends on residues near the extracellular face of the channel, influences canonical drug blockade, which occurs in proximity to residues in S6 that are nearer the cytoplasmic end of the channel's pore.

One possible explanation for this influence, which is concordant with the observations in this study, is that even low levels of inactivation (as seen in the single mutants at $+20$ mV) may be sufficient to stabilize the inhibition by drugs such as disopyramide. It is only when inactivation is almost completely eliminated (as in the case of the N588K/S631A double mutant at $+20$ mV, see Figure 2) that blockade of hERG by disopyramide is strongly attenuated. Although the effects of higher voltages on the block of N588K by the drugs used in this study were not investigated, such experiments would be valuable, as it might be predicted that, for drugs strongly dependent on inactivation, the gap between potency of inhibition of N588K and WT hERG might be smaller at more positive voltages. This is less likely to be the case, however, for drugs that appear weakly dependent on inactivation, and it is noteworthy that the modest effect of the single mutations on disopyramide and quinidine blockade of I_{hERG}, seen with the protocol used here, correlates well with evidence for clinical effectiveness of these agents in SQT1 patients (Wolpert *et al*., 2005; Schimpf *et al*., 2007).

The fact that disopyramide's potency is only marginally affected by either single mutation but is strongly compromised by the double mutation, is concordant with our observation of synergistic effects on inactivation by N588K and S631A, the latter providing evidence that hERG channel inactivation involves two synergistic processes (which are separately affected by mutations to the turret and outer mouth of the pore). It is possible that either one or both of the putative conformational changes can result in the stabilization of E-4031-induced blockade, whereas for disopyramide only one (but either one) of the synergistic processes at a time can stabilize blockade. The repositioning of S6 residues during the inactivation process in a way that optimizes interaction with drug molecules has been suggested as a possible mediator of the sensitivity of I_{hERG} blockade to channel inactivation (Chen *et al*., 2002). More specifically, the near equality of the effects of S631A and of N588K on inactivation and drug-induced inhibition with a range of compounds invites further investigation of whether one or both of the synergistic processes is required for the allosteric effects on S6. It is possible that mutation of either residue may be sufficient to interrupt a secondary process that merely finalizes inactivation, a process in which both amino-acid residues are necessary.

In conclusion, we have shown that different drugs have a range of sensitivities to inactivation attenuation, and we propose that in many cases this may explain why some drugs may be more useful than others for treating SQT1.

Acknowledgements

We gratefully acknowledge Lesley Arberry for technical support, Gabriela Quintero for the initial idea of the double mutant and the British Heart Foundation for generous financial support (PG/04/090/17460 & PG/06/139/21859).

Conflict of interest

The authors state no conflict of interest.

References

Alexander SP, Mathie A, Peters JA (2008). Guide to Receptors and Channels (GRAC), 3rd edition. *Br J Pharmacol* **153** (Suppl. 2): S1–S209.

Bellocq C, van Ginneken AC, Bezzina CR, Alders M, Escande D, Mannens MM *et al* (2004). Mutation in the *KCNQ1* gene leading to the short QT-interval syndrome. *Circulation* **109**: 2394–2397.

Brugada R, Hong K, Dumaine R, Cordeiro J, Gaita F, Borggrefe M *et al* (2004). Sudden death associated with short-QT syndrome linked to mutations in HERG. *Circulation* **109**: 30–35.

Chen J, Seebohm G, Sanguinetti MC (2002). Position of aromatic residues in the S6 domain, not inactivation, dictates cisapride sensitivity of HERG and eag potassium channels. *Proc Natl Acad Sci USA* **99**: 12461–12466.

Cordeiro JM, Brugada R, Wu YS, Hong K, Dumaine R (2005). Modulation of I_{Kr} inactivation by mutation N588K in *KCNH2*: a link to arrhythmogenesis in short QT syndrome. *Cardiovasc Res* **67**: 498–509.

Delgado C, Tamargo J, Henzel D, Lorente P (1993). Effects of propafenone on calcium current in guinea-pig ventricular myocytes. *Brit J Pharmacol* **108**: 721–727.

Duncan RS, McPate MJ, Ridley JM, Gao Z, James AF, Leishman DJ *et al*. (2007). Inhibition of the HERG potassium channel by the tricyclic antidepressant doxepin. *Biochem Pharmacol* **74**: 425–437.

Ficker E, Jarolimek W, Brown AM (2001). Molecular determinants of inactivation and dofetilide block in ether a-go-go (EAG) channels and EAG-related K^+ channels. *Mol Pharmacol* **60**: 1343–1348.

Ficker E, Jarolimek W, Kiehn J, Baumann A, Brown AM (1998). Molecular determinants of dofetilide block of HERG K^+ channels. *Circ Res* **82**: 386–395.

Gaita F, Giustetto C, Bianchi F, Schimpf R, Haissaguerre M, Calo L *et al*. (2004). Short QT syndrome: pharmacological treatment. *J Am Coll Cardiol* **43**: 1494–1499.

Gaita F, Giustetto C, Bianchi F, Wolpert C, Schimpf R, Riccardi R *et al*. (2003). Short QT Syndrome: a familial cause of sudden death. *Circulation* **108**: 965–970.

Gussak I, Brugada P, Brugada J, Antzelevitch C, Osbakken M, Bjerregaard P (2002). ECG phenomenon of idiopathic and paradoxical short QT intervals. *Card Electrophysiol Rev* **6**: 49–53.

Gussak I, Brugada P, Brugada J, Wright RS, Kopecky SL, Chaitman BR *et al*. (2000). Idiopathic short QT interval: a new clinical syndrome? *Cardiology* **94**: 99–102.

Hancox JC, Mitcheson JS (1997). Inhibition of L-type calcium current by propafenone in single myocytes isolated from the rabbit atrioventricular node. *Br J Pharmacol* **121**: 7–14.

Hancox JC, Witchel HJ, Varghese A (1998). Alteration of HERG current profile during the cardiac ventricular action potential, following a pore mutation. *Biochem Biophys Res Commun* **253**: 719–724.

Herzberg IM, Trudeau MC, Robertson GA (1998). Transfer of rapid inactivation and sensitivity to the class III antiarrhythmic drug E-4031 from HERG to M-eag channels. *J Physiol* **511**: 3–14.

Hong K, Bjerregaard P, Gussak I, Brugada R (2005a). Short QT syndrome and atrial fibrillation caused by mutation in *KCNH2*. *J Cardiovasc Electrophysiol* **16**: 394–396.

Hong K, Piper DR, Diaz-Valdecantos A, Brugada J, Oliva A, Burashnikov E *et al*. (2005b). *De novo KCNQ1* mutation responsible for atrial fibrillation and short QT syndrome *in utero*. *Cardiovasc Res* **68**: 433–440.

Lees-Miller JP, Duan Y, Teng GQ, Duff HJ (2000). Molecular determinant of high-affinity dofetilide binding to HERG1 expressed in *Xenopus* oocytes: involvement of S6 sites. *Mol Pharmacol* **57**: 367–374.

Levi AJ, Hancox JC, Howarth FC, Croker J, Vinnicombe J (1996). A method for making rapid changes of superfusate whilst maintaining temperature at 37 degrees C. *Pflügers Arch* **432**: 930–937.

Lu LX, Zhou W, Zhang X, Cao Q, Yu K, Zhu C (2006). Short QT syndrome: a case report and review of literature. *Resuscitation* **71**: 115–121.

McPate MJ, Duncan RS, Milnes JT, Witchel HJ, Hancox JC (2005). The N588K-HERG K^+ channel mutation in the 'short QT syndrome': mechanism of gain-in-function determined at 37 °C. *Biochem Biophys Res Commun* **334**: 441–449.

McPate MJ, Duncan RS, Witchel HJ, Hancox JC (2006). Disopyramide is an effective inhibitor of mutant HERG K^+ channels involved in variant 1 short QT syndrome. *J Mol Cell Cardiol* **41**: 563–566.

Milnes JT, Crociani O, Arcangeli A, Hancox JC, Witchel HJ (2003). Blockade of HERG potassium currents by fluvoxamine: incomplete attenuation by S6 mutations at F656 or Y652. *Br J Pharmacol* **139**: 887–898.

Mitcheson JS, Chen J, Lin M, Culberson C, Sanguinetti MC (2000). A structural basis for drug-induced long QT syndrome. *Proc Natl Acad Sci USA* **97**: 12329–12333.

Numaguchi H, Mullins FM, Johnson Jr JP, Johns DC, Po SS, Yang IC *et al*. (2000). Probing the interaction between inactivation gating and D-sotalol block of HERG. *Circ Res* **87**: 1012–1018.

Paul A, Witchel HJ, Hancox JC (2001). Inhibition of HERG potassium channel current by the class 1a antiarrhythmic agent disopyramide. *Biochem Biophys Res Commun* **280**: 1243–1250.

Paul AA, Witchel HJ, Hancox JC (2002). Inhibition of the current of heterologously expressed HERG potassium channels by flecainide and comparison with quinidine, propafenone and lignocaine. *Br J Pharmacol* **136**: 717–729.

Priori SG, Pandit SV, Rivolta I, Berenfeld O, Ronchetti E, Dhamoon A *et al*. (2005). A novel form of short QT syndrome (SQT3) is caused by a mutation in the *KCNJ2* gene. *Circ Res* **96**: 800–807.

Redfern WS, Carlsson L, Davis AS, Lynch WG, MacKenzie I, Palethorpe S *et al*. (2003). Relationships between preclinical cardiac electrophysiology, clinical QT interval prolongation and torsade de pointes for a broad range of drugs: evidence for a provisional safety margin in drug development. *Cardiovasc Res* **58**: 32–45.

Ridley JM, Milnes JT, Witchel HJ, Hancox JC (2004). High affinity HERG K^+ channel blockade by the antiarrhythmic agent dronedarone: resistance to mutations of the S6 residues Y652 and F656. *Biochem Biophys Res Commun* **325**: 883–891.

Robertson GA (2000). LQT2: amplitude reduction and loss of selectivity in the tail that wags the HERG channel. *Circ Res* **86**: 492–493.

Schimpf R, Veltmann C, Giustetto C, Gaita F, Borggrefe M, Wolpert C (2007). *In vivo* effects of mutant HERG K^+ channel inhibition by disopyramide in patients with a short QT-1 syndrome: a pilot study. *J Cardiovasc Electrophysiol* **18**: 1157–1160.

Schimpf R, Wolpert C, Bianchi F, Giustetto C, Gaita F, Bauersfeld U *et al*. (2003). Congenital short QT syndrome and implantable cardioverter defibrillator treatment: inherent risk for inappropriate shock delivery. *J Cardiovasc Electrophysiol* **14**: 1273–1277.

Schimpf R, Wolpert C, Gaita F, Giustetto C, Borggrefe M (2005). Short QT syndrome. *Cardiovasc Res* **67**: 357–366.

Smith PL, Baukrowitz T, Yellen G (1996). The inward rectification mechanism of the HERG cardiac potassium channel. *Nature* **379**: 833–836.

Teschemacher AG, Seward EP, Hancox JC, Witchel HJ (1999). Inhibition of the current of heterologously expressed HERG potassium channels by imipramine and amitriptyline. *Br J Pharmacol* **128**: 479–485.

Witchel HJ (2007). The hERG potassium channel as a therapeutic target. *Expert Opin Ther Targets* **11**: 321–336.

Witchel HJ, Dempsey CE, Sessions RB, Perry M, Milnes JT, Hancox JC *et al*. (2004). The low potency, voltage-dependent HERG blocker propafenone—molecular determinants and drug trapping. *Mol Pharmacol* **66**: 1201–1212.

Wolpert C, Schimpf R, Giustetto C, Antzelevitch C, Cordeiro J, Dumaine R *et al*. (2005). Further insights into the effect of quinidine in short QT syndrome caused by a mutation in HERG. *J Cardiovasc Electrophysiol* **16**: 54–58.

Yang BF, Xu DH, Xu CQ, Li Z, Du ZM, Wang HZ *et al*. (2004). Inactivation gating determines drug potency: a common mechanism for drug blockade of HERG channels. *Acta Pharmacol Sin* **25**: 554–560.

Zhang S, Zhou Z, Gong Q, Makielski JC, January CT (1999). Mechanism of block and identification of the verapamil binding domain to HERG potassium channels. *Circ Res* **84**: 989–998.

Zhou Z, Gong Q, Ye B, Makielski JC, Robertson GA, January CT (1998). Properties of HERG channels stably expressed in HEK 293 cells studied at physiological temperature. *Biophys J* **74**: 230–241.

Zou A, Xu QP, Sanguinetti MC (1998). A mutation in the pore region of HERG K^+ channels expressed in *Xenopus* oocytes reduces rectification by shifting the voltage dependence of inactivation. *J Physiol (London)* **509**: 129–137.